

SIMULTANEOUS SHIP-TO-SHIP INTERACTION AND BANK EFFECT ON A VESSEL IN RESTRICTED WATER

A Y Sian, A Maimun and Y Ahmed, Marine Technology Centre, Universiti Teknologi Malaysia, Malaysia
Rahimuddin, Universitas Hasanuddin, Indonesia

SUMMARY

The present study investigates the hydrodynamic interaction between two vessels, an LNG tanker and a container ship, advancing in parallel in the close proximity of a bank using an unsteady Reynolds-averaged Navier-Stokes (URANS) simulation. The study focused on the simultaneous effect of ship-ship interactions and the presence of the bank in the vicinity. Computations were carried out for the following various scenarios: (1) single ship bank effect, (2) two-ship interaction and (3) simultaneous effect of the bank and the presence of a nearby ship. Through a comparative CFD analysis, this study reveals the behaviours of the hydrodynamic forces and moments acting on the vessels and the changes in the flow field when the bank effect and ship-ship interaction complement each other. Apart from the CFD simulation, model tests were carried out for validation purposes. The overall results of the numerical simulation showed fairly good agreement with the experiment, though there was a high validation comparison error in some cases, indicating challenges in CFD prediction.

NOMENCLATURE

α	Bank slope (-)
B	Ship's breadth (m)
C_B	Block coefficient (-)
D	Experimental data value (-)
Fn	Froude number [U/\sqrt{gL}]
g	Acceleration of gravity (ms^{-2})
h	Water depth (m)
L_{pp}	Length between perpendiculars (m)
N	Yaw moment (Nm)
N'	Non-dimensional yaw moment (-)
o	Earth bound coordinate system (-)
ρ	Density of water (kg/m^3)
T	Ship's draft (m)
T_1	Draft of LNG ship (m)
T_2	Draft of S60 ship (m)
U	Ship's speed (ms^{-1})
X	Longitudinal force (N)
X'	Non-dimensional longitudinal force (-)
x, y, z	Coordinates in body axes (m)
Y	Sway force (N)
Y'	Non-dimensional sway force (-)
y^+	Non-dimensional wall distance (-)
y_b	Distance from the ship's centreline to the toe of the bank (m)
y_b/B	Distance from the ship's centreline to the toe of the bank over the ship breadth ratio (-)
y_{ss}	Lateral distance between midship (m)
y_{ss}/B	Lateral distance between midship over the ship breadth ratio (-)

1 INTRODUCTION

During the last decade, vessel size has been increasing to meet the demands of trade. Larger liquefied natural gas (LNG) carriers can meet the demand of energy. As a consequence, larger vessels are increasingly influenced

by waterway restrictions, which are further aggravated by the increase in marine traffic.

Features of restricted water, such as the presence of a sea bottom, the presence of a bank or the presence of other ships, can influence the behaviour of a vessel in operation, increasing the risk of marine disasters. Ship-to-ship interaction, for instance, can cause a ship to alter course. The forces from the interaction often draw ships together, resulting in a possible collision. Vessels operating in the close proximity of banks or lateral boundaries, however, may experience a lateral force and yaw moment, known as the bank effect, attracting the vessel to the bank because of asymmetric flow around the ship. The causes of these phenomena lie in the changes in the delicate balance of the pressure forces acting on a moving ship.

All of these hydrodynamic phenomena adversely modify the ship's manoeuvring behaviour. Thus, these hydrodynamic interactions have become important to consider for safe navigation, especially in restricted water, where vessels interact and experience hydrodynamic forces from shallow water, the bank effect, interaction between ships or a combination of these.

Information regarding all factors affecting the hydrodynamics effect in restricted water is vital for the safety of navigation. For this to be possible, the hydrodynamic forces between ships and the bank in restricted water should be properly understood. The realistic estimation and quantification of the hydrodynamics forces from the interaction in advance is important to the ship operator before the hydrodynamics forces lead to a disastrous event.

There have been a number of studies on the hydrodynamic behaviour of ships in restricted water, and they presented an important fundamental understanding to these phenomena. However, few studies have taken into account the simultaneous effects of shallow water, the bank

effect and ship-to-ship interactions, all which are linked in practice in restricted waters.

Most of the investigations of the interaction are on the bank effect or ship-ship interactions alone. Norrbin [1,2] experientially investigated the bank effects and obtained empirical expressions for the bank-induced lateral force and yaw moment for three different bank configurations, a vertical bank, a vertical submerged bank and a slope bank. Li et al. [3] extended the works of Norrbin [1,2] and focused on the bank effect in extremely shallow water ($h/T < 1.2$).

Vantorre et al. [4] performed a model test program on bank effects using a vertical surface-piercing bank and proposed empirical formulae for predicting the ship-bank interaction forces. Mathematical models for the estimation of the hydrodynamic forces, moment and ship sinkage by a sloped surface piercing bank and a bank with a submerged platform were given by Lataire and Vantorre [5].

Zou et al. [6] performed CFD analyses on a low-speed KVLCC2 tanker in a canal characterized by surface piercing banks. Zou and Larsson [7] provided a physical explanation of the bank effects in confined water.

Varyani et al. [8] and Varyani et al. [9] published empirical formulae to predict the sway force and yaw moment of a two-ship encounter and overtaking in a channel. Vantorre et al. [10] performed model tests with an auxiliary carriage installed in a towing tank to study the case of a ship meeting and overtaking. Varyani and Vantorre [11] presented semi-empirical generic models for calculation of the interaction forces acting on a moored ship based on slender body theory and experiments.

Lataire et al. [12] proposed mathematical models for the prediction of the surge force, sway force and yaw moment during a lightering manoeuvre. Zou and Larsson [13] conducted CFD computations on the ship-to-ship interaction in a lightering operation.

Fewer studies had considered the problems of the combined bank effect and ship interaction. Korsmeyer et al. [14] presented a three-dimensional panel method for the analysis of ship interactions applicable to a fluid domain bounded by irregular surfaces. Kijima and Yasukawa [15] examined the behaviour of hydrodynamic forces and the moment when two ships meet and overtake each other in a narrow water channel with vertical side walls using slender body theory. Kijima et al. [16] extended the study to the case of two ships in the proximity of a bank wall with semi-circle shape breakwater, a circular pier and an oval shaped pier. Kijima and Furukawa [17] discussed the effect of the ship's speed ratio for the case of ships running closely in the proximity of a bank wall with semi-circle shape breakwater and a circular pier.

The details of these hydrodynamic problems are worth examining further. The present work tries to gain insight into the interaction of ship-bank and ship-ship in shallow water and reveal the effect of various factors affecting the interaction. The focus of this study will be on vessel manoeuvring behaviour influenced by hydrodynamic interactions due to the bank effect and interaction with another ship nearby in restricted shallow water.

2 MODEL TESTS

2.1 TEST FACILITIES

The experiments in this study were conducted in the towing tank at the Marine Technology Centre (MTC) of Universiti Teknologi Malaysia (UTM). The tank has a total length of 120 m, a width of 4 m and a depth of 2.5 m. The towing carriage, equipped with a planar motion mechanism (PMM), can tow the ship models at speeds up to 5 m/s.

2.2 SHIP MODELS AND BANK GEOMETRIES

Two ship models have been used in this model test program. The main dimensions of the models are listed in Table 1. The primary ship model is a Tenaga Class LNG carrier scaled by a factor of 1:112. The performance and geometric properties of this specific model were published by Sian et al. [18] and Maimun et al. [19].

The secondary ship model used is an $L_{pp}=2.534$ m standard Series 60 $C_B=0.7$ hull form. The model was a single-screw merchant ship hull. This hull form is a classical model for ship hydrodynamics research with experimental data available in the literature. The body plans of both models are shown in Figures 1 and 2.

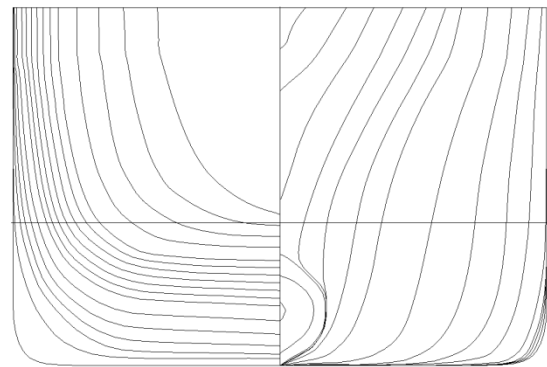


Figure 1. Body plan of the LNG carrier.

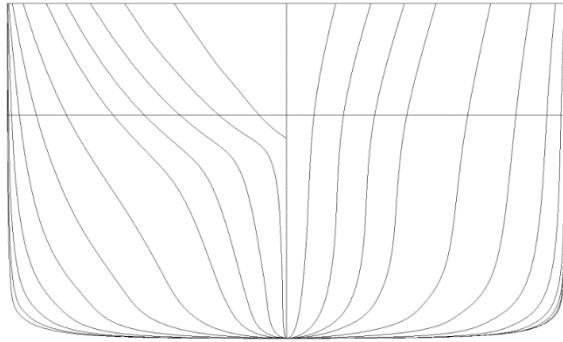


Figure 2. Body plan of the Series 60 model.

A 20-m shallow water platform was installed in the towing tank to investigate the shallow water effect. To investigate the bank effect, the bank of the submerged platform type was installed on top of the shallow water platform. The bank model composed a slope of 1/5, with a height of 0.08 m and a horizontal submerged part.

Table 1. Ship model dimensions

	LNG model	S60 model
Ship length, L_{pp}	2.375 m	2.534 m
Breadth, B	0.371 m	0.362 m
Draft, T	0.099 m	0.110 m
Block coefficient	0.746	0.7

2.3 MODEL TEST CONDITIONS

Water was drained from the tank to achieve the desired water height-to-LNG model's draught ratio of $h/T_1 = 1.2$, 1.4 and 1.6 during the test. The primary LNG model was attached to the computer controlled planar motion mechanism (PMM). The model was allowed to have pitch and roll but was restrained in the surge, sway and yaw motions. Two load cells were installed at the mechanical connectors.

The S60 model was mounted with a fixed frame at the towing carriage's working platform, allowing for the test of two ships travelling in parallel with no speed differences. The position of the working platform was flexible, allowing for lateral adjustment. The model was rigidly connected to the towing carriage. Thus, all motion of the model was restrained. No measurement was taken from the secondary model.

Both models were tested in an even keel without a rudder and propeller attached (Figure 3). The transversal position of the LNG ship model can be adjusted via a computer-controlled PMM, while the transversal position of second ship models can be manually adjusted by shifting the working platform.

The forces and moments on the LNG were measured with two strain gauge type load cells. The results presented in this study were obtained by averaging the measurements over the steady state conditions in the model tests for a distance of 1 to 2 ship lengths, which

were usually achieved after the ships travels for a distance of 2 to 5 ship lengths.

It must be noted that the h/T_1 ratio is computed based on the draft of the primary LNG model (0.099 m). Despite the best effort of the authors to perform the study with two models with identical size, the S60 model has approximately 10% extra ship draft at 0.110 m. At the $h/T_1 = 1.2$ condition, the gap beneath the model is essentially narrower for S60. For the S60 model, the water depth condition at $h/T_1 = 1.2$ is equal to $h/T_2 = 1.10$.

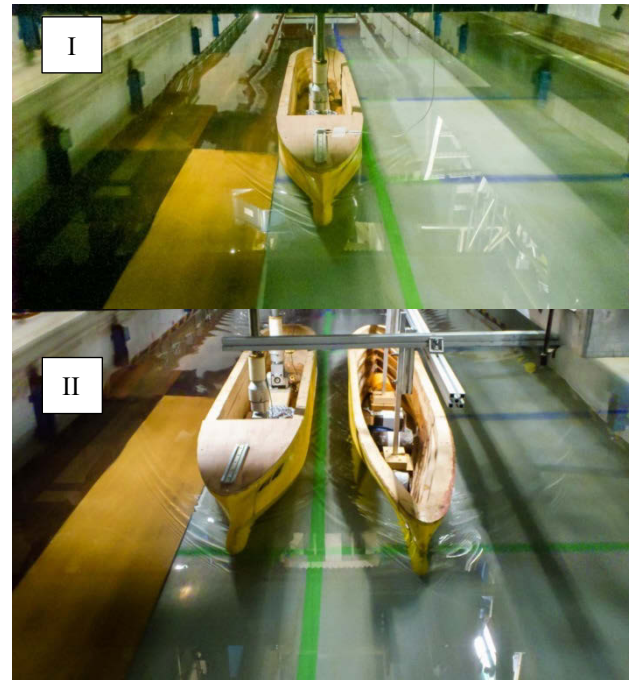


Figure 3. Captive model tests in the towing tank. I – Test on the bank effect in the shallow water condition and II – test on the two ships and bank effect.

2.4 CONVENTIONS AND REGISTRATION

The conventions and registration used in the tests are illustrated in Figure 4.

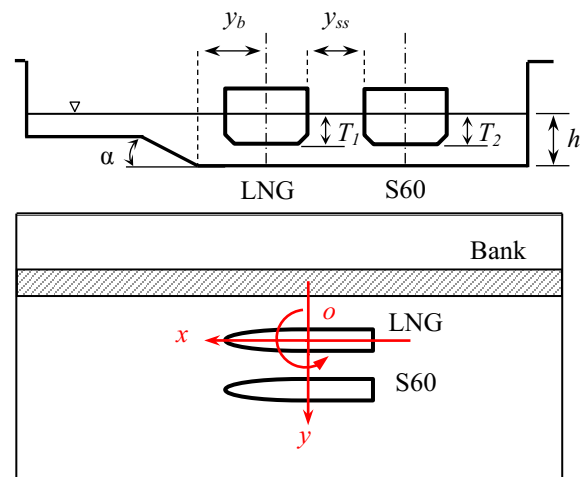


Figure 4. Test conventions and registrations.

2.5 NON-DIMENSIONALIZATION

The longitudinal force, sway force and yawing moment were non-dimensionalized using the following equations:

$$X' = \frac{X}{\frac{1}{2}\rho L^2 U^2} \quad (1)$$

$$Y' = \frac{Y}{\frac{1}{2}\rho L^2 U^2} \quad (2)$$

$$N' = \frac{N}{\frac{1}{2}\rho L^3 U^2} \quad (3)$$

3 NUMERICAL METHOD

3.1 GENERAL REMARKS

The hydrodynamic interactive forces and free surface flow in this study were examined using the general purpose CFD solver Fluent V15. The code solves incompressible unsteady Reynolds-averaged Navier-Stokes (URANS) computations by the finite volume method (FVM). The turbulence model used is the shear-stress transport (SST) $k-\omega$ model. The free surface in the CFD computations was tracked with the volume of fluid (VOF) model.

3.2 GRID GENERATION

The computational grids are generated by ICEM CFD by entirely using a structural grid approach. Some care has been taken in creating the grid. Finer grids are distributed at the region of the free surface and surrounding the ship hulls to resolve the flow gradients and to provide greater resolution about the free surface interface. The size of the first grid point away from ship hull was at approximately $y^+ = 50$, with 20 cells within the boundary layer to capture the detailed fluid property. The number of grid points used was approximately 2 million.

3.3 COMPUTATIONAL DOMAIN AND BOUNDARY CONDITIONS

Calculations were performed at the model scale. The computational domain was made up by seven boundaries: the hull surface, flow pressure inlet, flow pressure outlet, top, bottom and two side walls. A schematic diagram indicating the computational domain is given in Figure 5.

The dimensions of the hulls, tank bottom and two side walls of the domain correspond to the exact experiment set up in the towing tank. The length of the numerical towing tank was 11.5 m, and the ships were located 1.3 ship lengths of the slightly longer S60 model behind the

flow inlet and flow outlet at the aft of the two ship models at a distance of 2.3 ship lengths of S60.

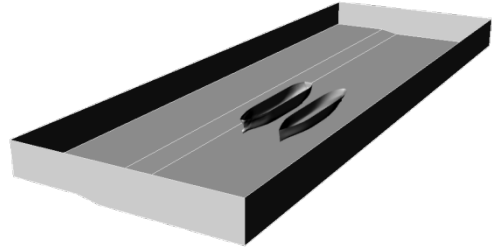


Figure 5. Overview of the computational domain.

Smooth walls and the no-slip condition were imposed for the hulls. The bank geometry and towing tank's wall were implemented as a moving wall to model the relative motion between the ground and ship model. A translational velocity identical to the flow inlet was imposed on the moving wall.

3.4 COMPUTATIONAL SETUP

The SIMPLE-Consistent algorithm was used for pressure-velocity coupling. The gradient discretization of the variables in the flow conservation equations was performed using the least squared cell-based method. Variables including the volume fraction, turbulent kinetic energy, dissipation rate and specific dissipation rate were discretized in time using the bounded second order implicit time integration transient formulation.

The pressure staggering option (PRESTO!) scheme was used for pressure interpolation in the discretization of the momentum equation, and the second-order upwind method was used for density interpolation in the discretization of the continuity equation. The turbulent kinetic energy and specific dissipation rate were discretized using the second-order upwind scheme. The volume fraction was discretized by the compressive scheme.

Simulations were performed with the free surface, and the ship models were fixed at an even keel for all cases. Simulations were performed in a time accurate manner to capture the unsteady flow features during hydrodynamic interactions, should they exist. The total physical time of 90 seconds was computed with the step size of 0.01 s.

Convergence was monitored by ensuring the ships' body forces and moments were stable. The convergence of each time step was to ensure that the residuals scaled by the initial imbalance of equations dropped three orders of magnitude, which was typically achieved in approximately 10-15 iterations during simulations. The simulation results were obtained by averaging the flow quantities over its statistical steady state.

The computations were conducted on a shared-memory type workstation. The computations employed four processors (3.6 GHz) and a total of 32 GB of 1600 MHz

DDR3 RAM. The computing time for each case required approximately 40 hours.

4 RESULTS AND DISCUSSION

4.1 CFD VALIDATION

The predicted sway force and yaw moment induced by the presence of the bank on the LNG were compared with the experimental data in Figure 6. The published bank effect formulations of Norrbin (1985) and Vantorre et al. (2002) for the sway force and yaw moment prediction were used to compare these values with the hydrodynamic force and moment in the current research.

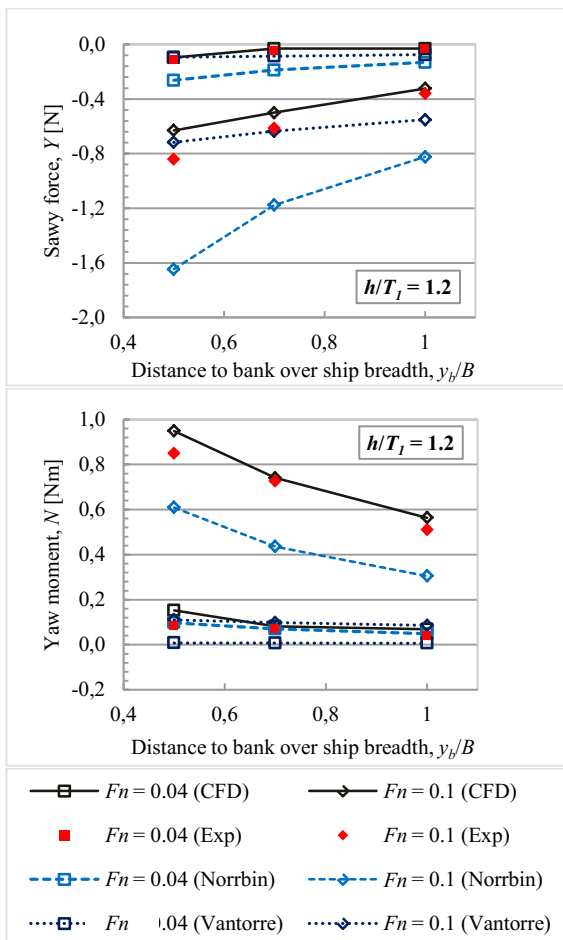


Figure 6. Sway force and yaw moment induced by the bank on the LNG at $h/T_1 = 1.2$ from the CFD analysis, the experiment, and the formulations of Norrbin (1985) and Vantorre et al. (2002).

For the ship-bank interaction, the agreement of the computed results and experiment measurement is generally satisfactory, with small deviations. The general tendency of the hydrodynamic force and moment by the experiments is well captured.

In general, CFD tends to under-predict the sway force and over-predict the yaw moment. The sway force of the LNG model is predicted with an average error at

16.21% D , the largest error being 30.46% D under-predicted and 0.91% D over-predicted. The yaw moments are all over-predicted, with an average error of 32.37% D , the largest error being 78.71% D .

The formulation of Norrbin [2] and Vantorre [10] over-predicted the sway force and yaw moment compared to the CFD model, as expected. The ship models used by Norrbin [2] and Vantorre [10] were tankers with a higher block coefficient compared to the LNG carrier in this research. Moreover, the expressions of Norrbin [2] were developed for a vertical submerged bank, whereas the formulations of Vantorre [10] were developed for a sloped surface piercing bank. Both bank models resulted in a higher blockage in the navigation channel compared to the bank model used in this research.

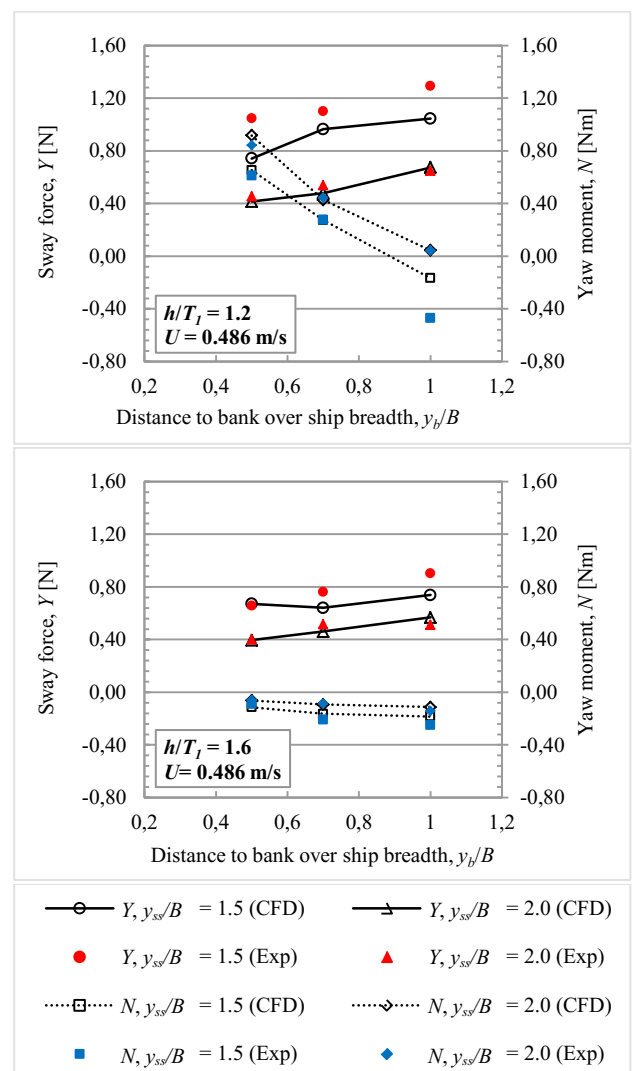


Figure 7. CFD predicted and measured sway force and yaw moment acting on the LNG ship model from simultaneous ship-bank and ship-ship interaction.

The predicted forces and moment in the simultaneous ship-bank and ship-ship interaction are compared with the experimental results in Figure 7. The sway forces are generally under-predicted, whereas the yaw moments are

over-predicted. The sway forces are predicted at an average error of 11.91%D, the largest error being 10.93%D over-predicted and 29.08%D under-predicted. The yaw moments are predicted at an average error of 16.43%D, the largest error being 27.52%D over-predicted and 64.49%D under-predicted. The changes in the sign for the yaw moment at $h/T_l = 1.2$, $y_b/B = 1$ and $y_{ss}/B = 1.5$ are successfully captured in the CFD computation. The overall computational results are encouraging, and the general tendency of the hydrodynamic force and moment by the experiments is well captured.

4.2 SHIP-BANK INTERACTION

Figure 8 shows the computed Y' and N' acting on the LNG model travelling in a straight course along the bank in shallow water for a wide range of Froude numbers and ship-bank distances. The interaction clearly shows where the model experiences a sway force, attracting the model to the bank, and the yaw moment pushed the ship bow away from the bank.

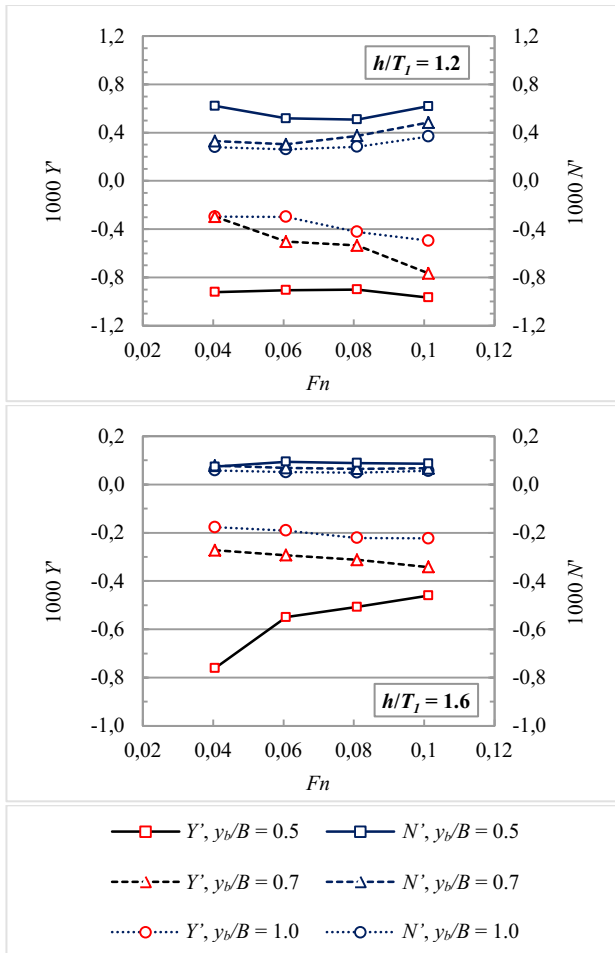


Figure 8. Computed Y' and N' induced by the bank on the LNG model.

The force and moment coefficients are made non-dimensional by the square of the ship speed. The curves obtained in the plots of the forces and moments over different Froude numbers indicate that the forces and

moment are not proportional to the speed squared, especially at $h/T_l = 1.2$. Straight horizontal lines should be obtained instead of a direct square proportion relationship.

Both the sway force and yaw moment are intensified at a lower h/T_l ratio. This is particularly the case for the yaw moment where a dramatic increment is observed when h/T_l approaches 1.2. The forces and moment are noticeably greater at a lower bank distance over the ship breadth ratio. The magnitude of the yaw moment is generally weaker compared to the sway force in the ship-bank interaction.

The expected transition of the sway force direction at an extremely low h/T ratio, as reported by Duffy [20] and Li et al. [3], was not demonstrated, probably because of the limited h/T_l condition tested, with 1.2 being the extreme water depth.

The test in a water depth of less than $h/T_l = 1.2$ or a ship closer to the bank at y_b/B less than 0.5 could not proceed without grounding the ship model.

4.3 SHIP-SHIP INTERACTION

The interaction of the two ships moving along parallel paths in shallow water is presented in this part. The problem considered here is limited to two approximately similar size vessels, the LNG model and S60, moving at a constant velocity with the midships aligned. Experimental data are not available for this part. Thus, only the numerical result presented. Figure 9 shows the predicted Y' and N' acting on LNG and S60 for several ship-bank distances at $Fn = 0.04$ and 0.1 and $h/T_l = 1.2$ and 1.6.

The interaction force and moment acting on the models were greater as the distances between the two ships decreased. Given that the gap between the ships becomes narrow at a lower y_{ss}/B , a more pronounced pressure drop was expected because of the accelerated flow. Therefore, a larger interactive sway force and yaw moment should be noted.

A higher magnitude of the sway force and yaw moment can be seen acting on the LNG at lower h/T_l ratio, except at $h/T_l = 1.2$, with a short distance between the two ships, where the magnitude decreased.

The numerical simulations have captured the effect of the reduction of the sway force, followed by changes in the force direction at small lateral distances between the ships, as reported by Fonfach et al. [21]. This is particularly the case for the LNG model at $y_{ss}/B = 1.5$ and $h/T_l = 1.2$. More of such sway force reduction phenomena are found in S60 because of its deeper ship draft.

At $Fn = 0.04$, the sway force changed from negative to positive, indicating that the force acting on the model changed from an attraction force to a repulsion force.

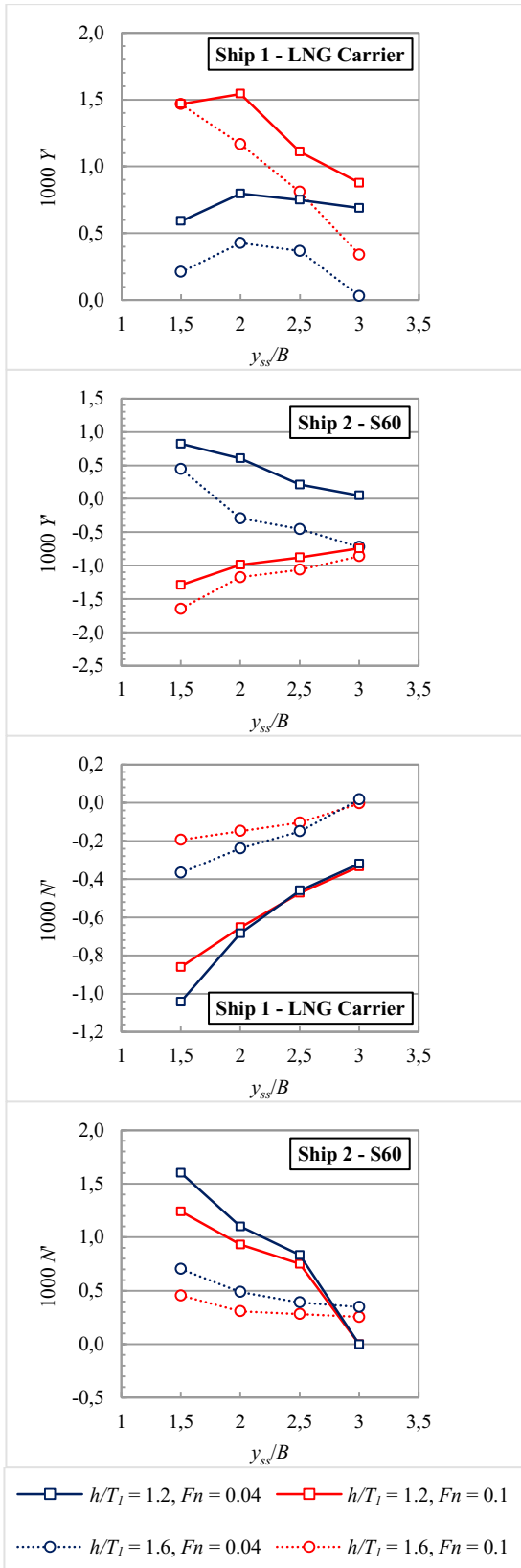


Figure 9. Computed Y' and N' induced on the LNG due to the interaction with the S60 ship model as a function of the lateral distance between the midships over the ship breadth ratio.

However, such a transition of the force direction was not seen in the LNG model. Such force transition phenomena have been reported by Duffy [20] and Li et al. [3] when the critical h/T ratio exceeds 1.10.

4.4 SIMULTANEOUS SHIP-BANK AND SHIP-SHIP INTERACTION

The interaction of two ships moving along parallel paths in the vicinity of the bank is presented in this part. The situation considered in the present study is where the LNG carrier model travel parallel with the S60 ship model at her port side and the submerged sloped bank at her starboard side.

Figure 10 shows the computed free surface elevations for a single ship in the shallow water condition, a single ship interacting with the bank, two ships interacting and a ship simultaneously interacting with the bank and the second ship at $Fn = 0.1$, $y_b/B = 1.0$ and $y_{ss}/B = 1.5$. The wave profiles along the hull are shown in Figure 11.

As seen in Figure 10, wave crests located at the zones of the high pressure at the ship bow are detected well by the CFD simulation. A great region of wave crests can be observed upstream of the ships, which could be attributed to stagnation.

A higher wave elevation and a greater region of wave crests upstream were observed in the case of simultaneous ship and bank interaction compared to the other two, which are responsible for the significant increase in the longitudinal force. Two peaks of the elevated water were observed between the bows of the two ships, which seem to be responsible for the bow out yaw moment induced on the two ships model.

Moving downstream, a wave trough attributed to Bernoulli's effect was observed over the length of the vessels. Careful observation shows the presence of two dips in the middle of the two ship models, which produce the attractive force between the two ships. In general, the free surface pattern between the two ships was similar for the two-ship interaction and the simultaneous bank and two-ship interaction, although the wave trough of the latter was more pronounced, indicating a stronger suction between the two ships.

An instantaneous snapshot of the free surface wave pattern at the starboard side of the LNG model during the experiment is shown in Figure 12. The computational results reproduce the trough and crest at the starboard and astern of the LNG model, very similar to the experimental results, and suggest that the wave elevation is well predicted by the CFD method.

A strong asymmetry of the free surface was observed in the ship-bank interaction cases. The wave trough at the starboard, followed by the wave crest astern of the starboard, suggests the presence of a lower pressure region

than the port side. A bow out yaw moment induced by the presence of the bank is expected because of the imbalance of the pressure field. This structure of the free surface at the starboard remains in the simultaneous ship-bank and two ship interactions, but there are distinct differences in the magnitude of wave elevation observed. The wave trough, followed by the wave crest, is noticeably more pronounced in the simultaneous two ship and bank interaction.

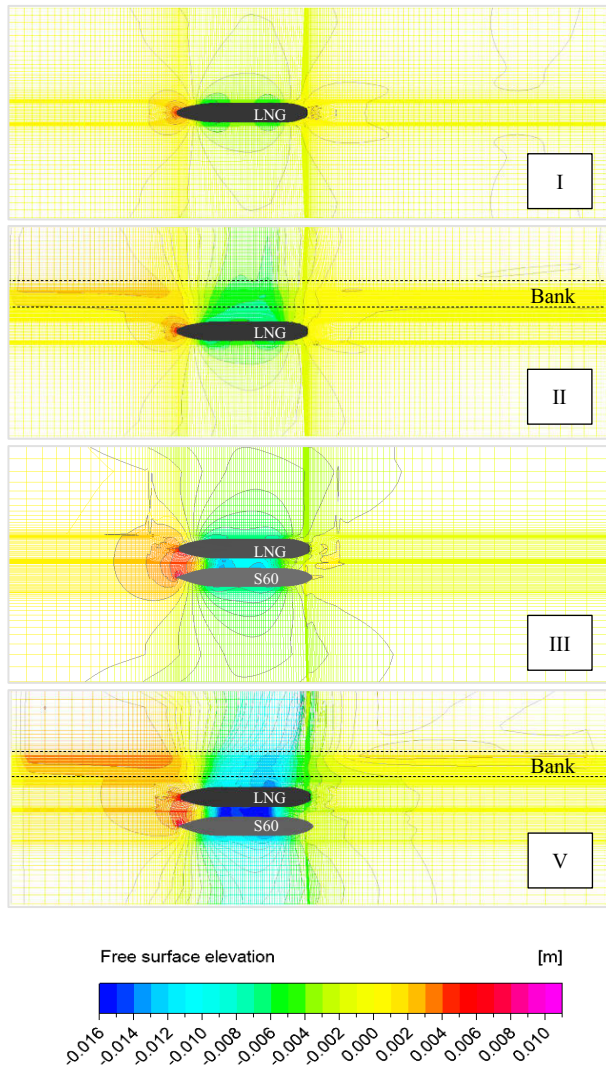


Figure 10. Computed free surface wave pattern at $h/T_1 = 1.2$. I – LNG model, II – LNG model with bank at the starboard, $y_b/B = 1.0$, III – Two-ship interaction, $y_{ss}/B = 1.5$, V – simultaneous two ship and bank interaction, $y_b/B = 1.0$, $y_{ss}/B = 1.5$.

The predicted X' , Y' and N' for the conditions of ship-bank interactions, two-ship interactions and simultaneous ship-bank and ship-ship interactions at $h/T_1 = 1.2$, 1.4 and 1.6 are given in Figure 13. Comparing the ship-bank interaction and the ship-ship interaction, the magnitudes of X' , Y' and N' from the ship-ship interaction alone were always greater than the magnitude induced by the ship-bank interaction alone.

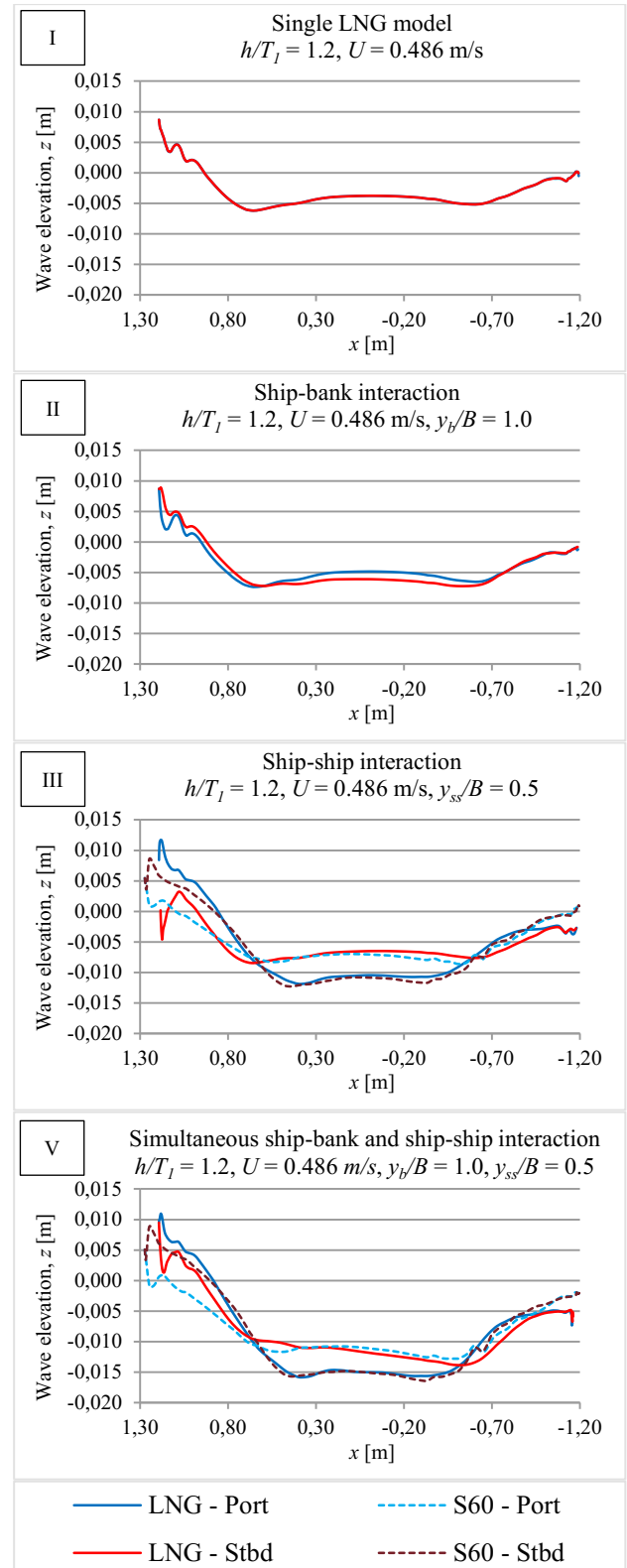


Figure 11. Computed wave profile along the hull at $h/T_1 = 1.2$. I – LNG model, II – LNG model with bank at the starboard, $y_b/B = 1.0$, III – two-ship interaction, $y_{ss}/B = 1.5$, V – simultaneous two ship and bank interaction, $y_b/B = 1.0$, $y_{ss}/B = 1.5$.

As discussed earlier, on the LNG carrier, the ship-bank interaction gives a negative Y' and positive N' , whereas

the ship-ship interaction gives a positive Y' and negative N' .

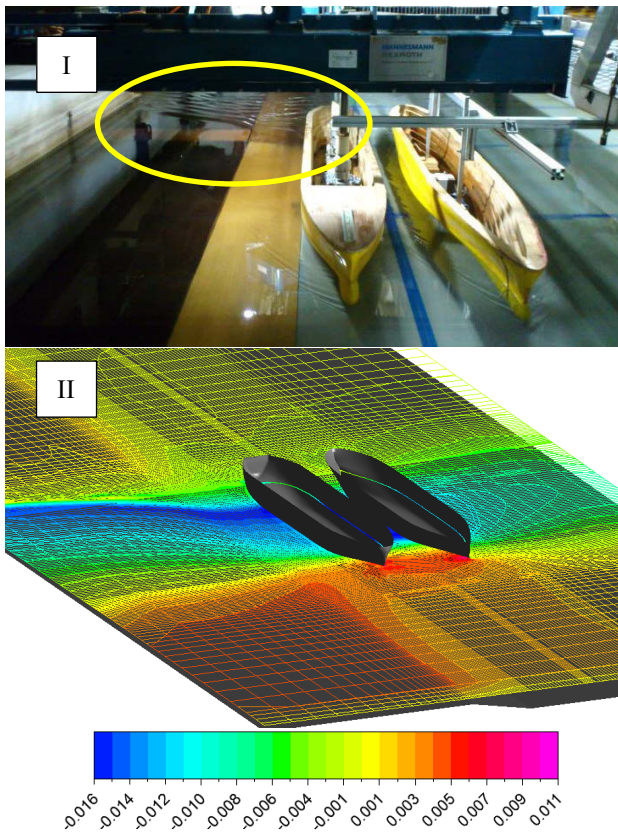


Figure 12. Comparison of the free surface wave pattern between the experimental and computational results, $h/T_1 = 1.2$, $y_b/B = 0.5$, $y_{ss}/B = 1.5$, $Fn = 0.1$. I – Experiment (the circle indicates a wave trough followed by a wave crest due to presence of the bank), II – CFD.

From Figure 13, it can be seen that the simultaneous ship-bank and ship-ship interactions resulted in a higher magnitude of X' compared to the magnitude from the ship-bank interaction or the ship-ship interaction alone, while the Y' and N' from the simultaneous ship-bank and ship-ship interactions were in the range of the two peak values from the bank or ships' interaction alone. X' increased rapidly between $h/T_1 = 1.2$ and 1.4 but dropped between $h/T_1 = 1.4$ and 1.6. For a specific distance from the bank, the magnitude of X' increased with shorter distances between the two ships.

Comparing the Y' and N' of the ship-bank interaction, the ship-ship interaction and simultaneous ship-bank and ship-ship interaction are all at their equal ship-ship or ship-bank distances at $y_b/B = 1.0$ and $y_{ss}/B = 1.5$. The resemblance of the Y' and N' direction in the simultaneous ship-bank and ship-ship interaction with the ship-ship interaction proved that the ships' interaction has more influence on the LNG compared to the bank effect. This conclusion agrees well with Kijima et al. [16], though different ships and bank models were used compared to the present paper.

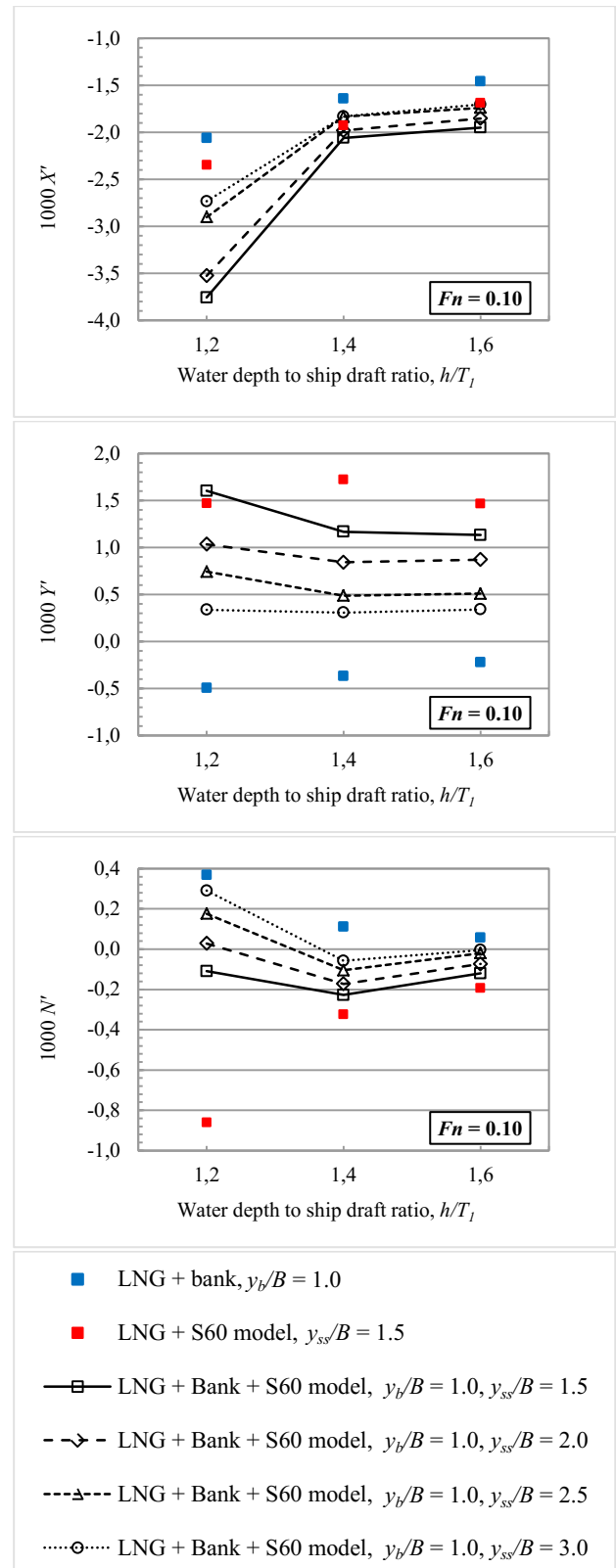


Figure 13. Computed X' , Y' and N' for the conditions of ship-bank interaction, two ship interaction and simultaneous bank and two ship interaction.

As seen in Figure 13, at a specific ship-bank distance at $y_b/B = 1.0$, a larger influence of the ship-ship interaction can be seen on Y' , where the LNG is attracted to the S60

model at y_{ss}/B lower than 2.0. At $y_{ss}/B = 2.5$, the resultant effect of the bank and ships interaction resulted in Y' being close to zero. At $y_{ss}/B = 3.0$, Y' acts in a different direction, and a higher influence of the bank effect can be seen where the LNG is attracted to the bank.

N' behaves in a different way compared to Y' . At a specific ship-bank distance at $y_b/B = 1.0$, the negative N' acted on the LNG for all cases at $h/T_l = 1.4$ and 1.6 , indicating that the influence of the ship-ship interaction is dominant and the ship bow swings toward the bank. At $h/T_l = 1.2$, however, a positive N' is seen in all cases except at $y_{ss}/B = 1.5$.

Preliminary computations have indicated the sway forces and yaw moments from the ship-bank interaction and the ship-ship interaction seem to superpose and counteract each other, but these effects will require further investigation.

5 FUTURE WORKS

It has been shown that computations on simultaneous ship-bank and ship-ship interactions yield results that are in good agreement with the measured data. In all cases, the results presented were for two ships moving at a zero speed difference and zero longitudinal distances without a rudder and propeller. In addition, ship motion such as sinkage and trim were not included. Additional investigations on the influence of these factors are needed for a more realistic understanding of ships and bank interactions in restricted waters.

6 CONCLUSIONS

This paper presented an investigation of the hydrodynamic interaction between two vessels, an LNG tanker and an S60 container ship, advancing in parallel in close proximity of submerged sloped bank in restricted shallow water. Computations conducted for various scenarios, including (1) the single ship bank effect, (2) the two-ship interaction and (3) the simultaneous effect of the bank and the presence of a nearby ship, have provided deeper insight into the hydrodynamics of simultaneous ship-ship and ship-bank interaction.

The CFD model successfully simulated the wave pattern, and the computed results show fairly good agreement with the experimental data. The correlation between the experimental and computed results indicated adequately reliable estimates of the hydrodynamic interaction forces and moment obtained. Changes in the flow field on the ships when the bank effect and ship-ship interaction complement each other were also revealed.

The main conclusions are as follows:

- The combination of the ship-bank and ship-ship interactions resulted in a higher longitudinal

force compared to ship-ship or ship-bank interactions alone.

- At a fixed ship-bank and ship-ship distances, the presence of the second ship has more influence compared to the bank effect.
- The interaction effects are amplified at a low water depth.
- The sway forces and yaw moments from the ship-ship interaction and the ship-bank interaction acted on a ship from the opposite direction and offset each other. The magnitude of the simultaneous ship-bank and ship-ship interaction lie between the values of the ship-bank interaction and the ship-ship interaction.

7 ACKNOWLEDGEMENTS

The presented work is supported by the Marine Technology Center (MTC) and Centre for Information and Communication Technology (CICT) in Universiti Teknologi Malaysia.

8 REFERENCES

1. Norrbin, N. (1974) Bank effects on a ship moving through a short dredged channel, *10th ONR Symposium on Naval Hydrodynamics*, Cambridge.
2. Norrbin, N. (1985) Bank clearance and optimal section shape for ship canals, *26th PIANC International navigation Congress*, Brussels.: pp. 167-178.
3. Li, D. Q.; Leer-Andersen, M.; Ottoson, P.; Tragardh, P. (2001). Experimental investigation of bank effects under extreme conditions. *Proceedings of Practical Design of Ships and Other Floating Structures (PRADS)*, Shanghai, China.: pp. 541-546.
4. Vantorre, M.; Delefortrie, G.; Eloit, K.; Laforce, E. (2003). Experimental investigation of ship-bank interaction forces. *Proceedings of The International Conference on Marine Simulation and Ship Maneuverability (MAR-SIM)*, Kanazawa.: pp. 311-319.
5. Lataire, E.; Vantorre, M. (2008). Ship-bank interaction induced by irregular bank geometries. *Proceedings of 27th Symposium on Naval Hydrodynamics*, Seoul, Korea.
6. Zou, L.; Larsson, L.; Delefortrie, G.; Lataire, E. (2011). CFD prediction and validation of ship-bank interaction in a canal. *Proceedings of the Second International Conference on Ship Manoeuvring in Shallow and Confined Water: Ship to Ship Interaction*. 18-20 May. Trondheim, Norway.: pp. 413-422.
7. Zou, L.; Larsson, L. (2013). Confined Water Effects on the Viscous Flow around a Tanker with Propeller and

- Rudder. *International Shipbuilding Progress*. 60: pp. 309-343.
8. Varyani, K. S.; McGregor, R. C.; Krishnankutty, P.; Thavalingam, A. (2002). New Empirical and Generic Models to Predict Interaction Forces for Several Ships in Encounter and Overtaking Manoeuvres in a Channel. *International Shipbuilding Progress*. 49(4): pp. 237-262.
9. Varyani, K. S.; Thavalingam, A.; Krishnankutty, P. (2004). New Generic Mathematical Model to Predict Hydrodynamic Interaction Effects for Overtaking manoeuvres in Simulators. *Journal of Marine Science and Technology*. 9: pp. 24-31.
10. Vantorre, M.; Verzhbitskaya, E.; Laforce, E. (2002). Model Test Based Formulations of Ship-Ship Interaction Forces. *Ship Technology Research*. 49: pp. 124-137.
11. Varyani, K. S.; Vantorre, M. (2006). New Generic Equation for Interaction effects on a Moored Container-ship Due to a Passing Tanker. *Journal of Ship Research*. 50(3): pp. 278-287.
12. Lataire, E.; Vantorre, M.; Delefortrie, G.; Candries, M. (2012). Mathematical Modelling of Forces Acting on Ships during Lightering Operations. *Ocean Engineering*. 55: pp. 101-115.
13. Zou, L.; Larsson, L. (2013). Numerical Predictions of Ship-to-Ship Interaction in Shallow Water. *Ocean Engineering*. 72: pp. 386-402.
14. Korsmeyer, F. T.; Lee, C. H.; Newman, J. N. (1993). Computation of Ship Interaction Forces in Restricted waters. *Journal of Ship Research*. 37(4): pp. 298-306.
15. Kijima, K.; Yasukawa, H. (1984) Manoeuvrability of Ships in Narrow Waterway. *J Soc Nav Archit Jpn*. 156: pp. 25-37.
16. Kijima, K.; Furukawa, Y.; Qing, H. (1991). The Interaction Effects between Two Ships in the Proximity of Bank Wall. *Trans. Of the West-Japan Society of Naval Architects*. 81: pp. 101-112.
17. Kijima, K.; Furukawa, Y. (1994). A ship manoeuvring motion in the proximity of pier. *Proceedings of the International Committee on Manoeuvring and Control of Marine Craft (MCMC)*. Southampton.: pp. 211-222.
18. Sian, A. Y.; Maimun, A.; Priyanto, A.; Ahmed, Y. M.; Nakisa, M.; Rahimuddin. (2014). Numerical Investigation for Resistance Characteristics of LNG Carrier. *Jurnal Teknologi*. 67(9): pp. 101-107.
19. Maimun, A.; Priyanto, A.; Rahimuddin; Sian, A. Y.; Awal, Z. I.; Celement, C. S.; Nurcholis; Waqiyuddin, M. (2013). A Mathematical Model on Manoeuvrability of a LNG Tanker in Vicinity of Bank in Restricted Water. *Safety Science*. 53: pp. 34-44.
20. Duffy, J. T. (2002). *Prediction of bank induced sway force and yaw moment for ship handling simulator*. Australian Maritime College, Australia.
21. Fonfach, J. M. A.; Sutulo, S.; Soares, C. G. (2011). Numerical study of ship-to-ship interaction forces on the basis of various flow models. *Proceedings of the Second International Conference on Ship Manoeuvring in Shallow and Confined Water: Ship to Ship Interaction*, Trondheim, Norway.: pp. 137-146.

9 AUTHORS' BIOGRAPHIES

A. Y. Sian is currently a Ph.D. student at the Marine Technology Centre, Universiti Teknologi Malaysia. He received his BSc (Maritime Technology) from Universiti Malaysia Terengganu, Malaysia. His research interests include manoeuvring in shallow water, bank effects and ship-to-ship interactions.

A. Maimun is a Professor at the Marine Technology Centre, Universiti Teknologi Malaysia. He received his BSc in 1983, MSc in 1985 and Ph.D. from Strathclyde University, Glasgow, in naval architecture and ocean engineering. His research interests include ship dynamic stability, ship simulator, seakeeping, manoeuvring, offshore structures dynamics and fast craft design.

Y. Ahmed is currently a senior lecturer at Universiti Teknologi Malaysia, Malaysia. He received his Ph.D. from Alexandria University, Egypt. His research interests include ship hydrodynamics and computational fluid dynamics (CFD).

Rahimuddin is currently a lecturer at Universitas Hasanuddin, Indonesia. He obtained his Ph.D. from Universiti Teknologi Malaysia.